Published in Advances in Water Resources, 29, issue 8, 1140-1154, 2006
which should be used for any reference to this work

Direct simulation of solute recycling in irrigated areas

Ellen Milnes *, Pierre Perrochet [1]

Université de Neuchâtel, Rue Emile-Argand 11, CH-2007 Neuchâtel, Switzerland

Abstract

Solute recycling from irrigation can be described as the process that occurs when the salt load that is extracted from irrigation wells and distributed on the fields is returned to the groundwater below irrigated surfaces by deep percolation. Unless the salt load leaves the system by means of drains or surface runoff, transfer to the groundwater will take place, sooner or later. This can lead to solute accumulation and thus to groundwater degradation, particularly in areas where extraction rates exceed infiltration rates (semi-arid and arid regions). Thus, considerable errors can occur in a predictive solute mass budget if the recycling process is not accounted for in the calculation. A method is proposed which allows direct simulation of solute recycling. The transient solute response at an extraction well is shown to be a superposition of solute mass flux contributions from n recycling cycles and is described as a function of the travel time distribution between a recycling point and a well. This leads to an expression for a transient 'recycling source' term in the advection–dispersion equation, which generates the effect of solute recycling. At long times, the 'recycling source' is a function of the local capture probability of the irrigation well and the solute mass flux captured by the well from the boundaries. The predicted concentration distribution at steady state reflects the maximum spatial concentration distribution in response to solute recycling and can thus be considered as the solute recycling potential or vulnerability of the entire domain for a given hydraulic setting and exploitation scheme. Simulation of the solute recycling potential is computationally undemanding and can therefore, for instance, be used for optimisation purposes. Also, the proposed method allows transient simulation of solute recycling with any standard flow and transport code.

Keywords: Solute recycling; Irrigation salinity; Transfer function theory; Transport modelling

1. Introduction

Solute recycling in irrigated areas can be described as the salinity observed in the groundwater caused by redistribution of the extracted salt load from the aquifer onto irrigated fields and subsequent transfer to the groundwater by deep percolation. Depending on the fraction of applied water that leaves the system by evapotranspiration, the concentration of the irrigation return flow can be several times larger than that of the applied irrigation water [25,27,28]. For plant growth, flushing of solutes below the root zone is crucial, and for economic reasons, minimising the fraction of deep percolation is important [33]. As an example, Aragüés et al. [2] estimated that one hectare of irrigated crop land in the Ebro Valley in Spain yields 20 tons of salt per year.

One of the main problems that irrigated agriculture faces today is the challenge of providing food to a growing population with increasingly poor water quality. Water quality degradation due to solute recycling is a major consequence of constrained irrigation schemes, particularly in semi-arid and arid regions with intensive

* Corresponding author. Tel.: +41 32 718 2677.
E-mail addresses: ellen.milnes@unine.ch (E. Milnes), pierre.perrochet@unine.ch (P. Perrochet).
[1] Tel.: +41 32 718 2577.

agriculture [24]. Beltrán [5] pointed out that optimal soil salinity control is not necessarily the optimal groundwater or surface water salinity control. Therefore, he suggests that the different effects of solute recycling from irrigation require management solutions, which exceed the field and farm scale. Since the highest priority for irrigation schemes is to comply with economic constraints (maximising crop production and minimising irrigation costs), groundwater issues should not be neglected. Authors such as Tanji [30], Aragüés et al. [2], Konikow and Person [20], Bouwer [6,7], Close [9], Beke et al. [4], Prendergast et al. [26] and Al-Senafy and Abraham [1] have focused on the establishment of solute mass budgets, on the quantification of the mechanisms of solute recycling, solute mass loading of the unsaturated zone and on groundwater contamination due to irrigation practices.

Authors such as Vengosh et al. [34,35], Kolodny et al. [19] and Kim et al. [18] have developed geochemical techniques allowing identification of, and distinction between, different salinisation processes, including solute recycling from irrigation. Using such geochemical techniques, Cardona et al. [8] identified three superimposed salinisation mechanisms in a coastal aquifer in Mexico, and found that solute recycling from irrigation was the most important process. However, groundwater was managed in the belief that seawater intrusion was the main cause of groundwater quality degradation, which implied landward displacement of salt-affected wells. These were rapidly affected by salinisation again, since solute recycling and not seawater intrusion was the main salinisation mechanism. This example illustrates that correct identification of different salinisation processes is crucial for the design of adequate groundwater management schemes.

Numerical models have often been used for management purposes, such as evaluation of future salinity distributions in seawater intruded aquifers, optimisation of well extraction rates and irrigation schemes or delimitation of capture zones [3,11,12,14,22,36]. Since solute recycling is a function of the solute mass flux extracted from irrigation wells, it is not included as a standard option in commercial software packages and is therefore rarely quantified. Solute recycling from irrigation might not always be of importance, but in areas where irrigation rates exceed infiltration rates (e.g., semi-arid and arid regions) its impact should be evaluated. Neglecting solute recycling in areas where extracted groundwater is highly mineralised (e.g., in seawater intruded settings) may lead to a significant error in the solute mass balance. Milnes and Renard [21] carried out two numerical simulation scenarios for the same coastal aquifer, with and without solute recycling, showing important differences in the predicted concentration distributions. The result obtained with the simulation scenario with solute recycling compared well with field observations.

The main objectives of the present work are the development of a procedure that allows simulation of solute recycling with standard simulation codes and a process-based assessment of the spatial salinisation potential related to solute recycling in arbitrary systems. For this purpose, a distributed 'recycling source' term in the advection–dispersion equation is first defined. Then, in order to predict this coupled 'recycling source', the recycling process is described mathematically, making use of the transfer function theory [15–17] and transit time probability density functions [10,22]. The transient solute recycling response at an extraction well is treated as a superposition of solute mass flux contributions from n possible recycling cycles and is obtained from the convolution integral of the recycling transfer function (RTF) with the solute mass captured by the wells from the boundaries. This allows prediction of the distributed 'recycling source' term in the advection–dispersion equation (ADE) in a pre-processing stage, followed by direct simulation of solute recycling. The thereby predicted concentration distribution at long times reflects the maximum concentration in response to solute recycling and is interpreted as solute recycling potential or vulnerability of the entire domain for the given hydraulic setting. In a similar way to Goode [13], who showed that the distribution of mean groundwater age obeys the solute-transport equation with a distributed zero-order source of unit strength, corresponding to the rate of aging, we show that a solute source in the steady state form of the ADE can be defined to generate the effect of solute recycling at long times, being a function of the local capture probability and the solute mass flux contribution to the well from the boundaries. This long-time behaviour is illustrated on homogeneous and heterogeneous examples, and the 'recycling source' is expanded to systems with several extraction wells and irrigation plots. Since the steady state approach is computationally undemanding, the potential use of the proposed simulation procedure for optimisation purposes is illustrated on an example.

2. General description of the solute recycling process in arbitrary systems

The main difficulty in describing the solute recycling process is that the water and solute cycles are partly disconnected (Fig. 1). If the solute mass flux applied with the irrigation water does not leave the system by means of drains or surface runoff, it is sooner or later transferred to the groundwater below the irrigation surfaces by deep percolation, while the applied irrigation water will partly leave the system by evapotranspiration. Even if irreversible chemical processes and plant solute uptake can be neglected, processes taking place in the

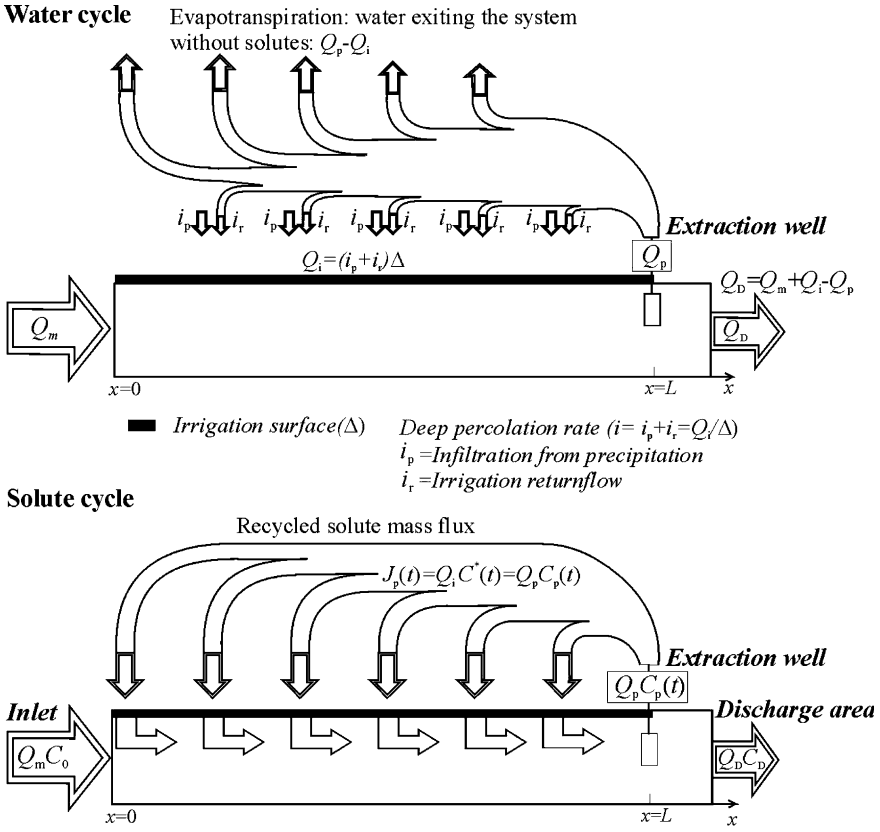

Fig. 1. Schematised irrigated system with one inlet boundary (at $x = 0$), an extraction well (at $x = L$) which is used for irrigating the surface Δ and a regional discharge area. The differences in the water and solute cycles are induced by evaporative losses.

unsaturated zone will influence the short-term and medium-term groundwater quality degradation (e.g., [23,29, 32]). If the soil acts as good buffer between the root zone and the groundwater, soil salinity will increase, while groundwater salinisation will be slowed down. On the other hand, poor soil buffers with fast transfer will more rapidly affect the groundwater, since solutes are not stored. However, if transport in the unsaturated zone is conservative, the long-term mass balance in the groundwater remains unchanged.

Fig. 1 schematises an aquifer system in hydraulic steady state condition with one extraction well, a lateral inflow boundary and a regional discharge area. The unsaturated zone is neglected, although the following considerations can easily be extended to include the effect of the unsaturated zone. An irrigation plot Δ [L^2] is schematised between the inlet ($x = 0$) and the extraction well ($x = L$), on which the extracted solute mass flux from the extraction well is distributed with the applied irrigation water. In Fig. 1, Q_m [$L^3\,T^{-1}$] is the lateral inflow with a concentration $C_0 > 0$ [$M\,L^{-3}$], while Q_p [$L^3\,T^{-1}$] stands for the well extraction rate with $C_p(t)$ being the concentration of the extracted water. Q_D [$L^3\,T^{-1}$] denotes the regional discharge rate with a concentration $C_D(t)$ [$M\,L^{-3}$]. C^* is the concentration of the deep percolation Q_i [$L^3\,T^{-1}$], consisting of the irrigation return flow ($i_r\Delta$) and the effective infiltration from precipitation ($i_p\Delta$).

In a system like that shown in Fig. 1, the extracted solute mass flux $J_p(t) = Q_pC_p(t)$ is transferred to the groundwater by deep percolation Q_i. If all the extracted water is used for irrigation, the difference between the water and the solute cycles is caused by evaporative losses, leaving solutes behind. The ratio of the deep percolation Q_i and the extraction rate Q_p will determine whether solute recycling will lead to an increase in groundwater salinity. If deep percolation is smaller than the extraction rate, the average system concentration will increase, since the water deficit induced by evaporative losses will be compensated by lateral inflow, conveying solutes into the system. If the deep percolation Q_i equals or exceeds the extraction rate Q_p, the average system concentration will not increase, since no solutes are conveyed into the system along the lateral boundary, i.e., the salt-load is exported out of the system. Hence, the main prerequisite for groundwater salinisation by solute recycling is that extraction rates exceed infiltration rates. Such conditions are typically found in arid and semi-arid regions, where pan evaporation is high and deep percolation small.

3. Definition of a distributed 'recycling source' term in the advection–dispersion equation

The solute mass flux that is introduced into the system by solute recycling can be considered as a solute 'recycling source' term RS [M L^{-2} T^{-1}] that can be introduced in the 2-D advection–dispersion equation as follows:

$$\frac{\partial e\phi C}{\partial t} = -\nabla \cdot (e\mathbf{q}C - \phi e\mathbf{D}\nabla C) + \mathrm{RS}, \tag{1}$$

where ϕ [–] is the saturated porous volume, e [L] the aquifer thickness, C [M L^{-3}] the concentration, $\mathbf{q}$ [L T^{-1}] the specific flux vector, and $\mathbf{D}$ [L^2 T^{-1}] the dispersion tensor. The 'recycling source' term RS in Eq. (1) can easily be extended to unsaturated/saturated problems and to 3-D systems by re-introducing the extracted solute mass flux into a recycling volume.

Assuming that no solutes are lost from the system and that irrigation takes place with groundwater extracted from the underlying aquifer, the solute mass that is re-introduced into the system by solute recycling equals the extracted solute mass flux $J_\mathrm{p}(t) = Q_\mathrm{i}C^*(t) = Q_\mathrm{p}C_\mathrm{p}(t)$ from the irrigation well. The distributed 'recycling source' RS in Eq. (1) can then be expressed in terms of the extracted solute mass flux as follows:

$$\mathrm{RS}(t) = \frac{Q_\mathrm{i}C^*(t)}{\Delta} = \frac{Q_\mathrm{p}C_\mathrm{p}(t)}{\Delta} = \frac{J_\mathrm{p}(t)}{\Delta} \tag{2}$$

where $J_\mathrm{p}(t)/\Delta$ [M L^{-2} T^{-1}] is the 'recycling source' RS(t) in Eq. (1) that is applied on the irrigated surface Δ (elsewhere in the domain: RS(t) = 0).

Numerically, Eq. (1) can be solved by evaluating the extracted solute mass flux $J_\mathrm{p}(t)$ in Eq. (2) at each time-step and re-introducing it as a distributed solute source on the designated irrigation plot Δ. To solve this in an automatic way, solute recycling has to be implemented in a simulation code with a time-stepping procedure. Otherwise, simulation of solute recycling may be very time-consuming, requiring interruption of the simulation to evaluate the extracted solute mass flux and to 'manually' adapt the solute sources (e.g., [21]).

In the following, the extracted solute mass flux $J_\mathrm{p}(t)$ in Eq. (2) will be evaluated in a pre-processing stage by means of the transfer function theory, in order to de-couple the 'recycling source' in Eq. (1).

4. Application of the transfer function theory to solute recycling

In an arbitrary advective–dispersive system in hydraulic steady state, a transfer function exists from every point within the system to any observation point, e.g., an extraction well [15,17]. The transfer function between any point $\boldsymbol{x}$ in a domain and the observation point $\boldsymbol{x}'$ describes how an input signal released at the inlet point $\boldsymbol{x}$ will be transformed by the time of arrival at the extraction well $\boldsymbol{x}'$. The transfer function corresponds to the travel time PDF, describing the distribution of solute life times τ_life, conditional on the τ_in, the time at which solutes entered the system [16]. According to the transfer function theory [15,17], the transfer function reflects the internal dynamics between an inlet and an observation point (e.g., well) and is defined as the response of the system to a narrow pulse input at inlet:

$$J_\mathrm{p}(t) = Q_\mathrm{p}C_\mathrm{p}(t) = \int_0^t g_t^\gamma(\tau_\mathrm{in})\delta(\boldsymbol{x}, t-\tau_\mathrm{in})m^*\,\mathrm{d}\tau_\mathrm{in} = m^* g_t^\gamma(t), \tag{3}$$

where $g_t^\gamma(t) = g_t(\boldsymbol{x}'|t, \boldsymbol{x}, \tau_\mathrm{in})$ [T^{-1}] is the travel time PDF between the injection point at the cartesian coordinates $\boldsymbol{x}$ and the extraction well $\boldsymbol{x}'$, and m^* [M] is the mass released at $\boldsymbol{x}$. The flow paths between $\boldsymbol{x}$ and $\boldsymbol{x}'$ are symbolised by the index γ in $g_t^\gamma(t)$. The travel time PDF $g_t^\gamma(t)$ is the product of the well extraction rate Q_p [L^3 T^{-1}] and the flux concentration $C_\mathrm{p}(t)$ [M L^{-3}] at the well, corresponding to the well solute mass response $J_\mathrm{p}(t)$ [M T^{-1}] to an instantaneous mass release at inlet $\boldsymbol{x}$. Hence, for a unit mass input of $m^* = 1$, the solute mass response $J_\mathrm{p}(t)$ at the irrigation well equals the travel time PDF $g_t^\gamma(t)$, with its integral corresponding to the probability $P(\boldsymbol{x})$ of a solute injected at $\boldsymbol{x}$ being captured by the well at $\boldsymbol{x}'$ as follows [17]:

$$P(\boldsymbol{x}) = \int_0^\infty g_t^\gamma(t)\,\mathrm{d}t. \tag{4}$$

Transfer functions, as described by Eq. (3), are used to model output flux signals at an observation point $\boldsymbol{x}'$ (e.g., a well) as a function of any given input flux released at a point $\boldsymbol{x}$. According Jury and Roth [17], the output flux $J_\mathrm{p}(t)$ at the well results from the convolution integral of the input signal $I(\boldsymbol{x}, t)$ with the transfer function $g_t^\gamma(t)$ as follows:

$$J_\mathrm{p}(t) = Q_\mathrm{p}C_\mathrm{p}(t) = \int_0^t g_t^\gamma(\tau_\mathrm{in})I(\boldsymbol{x}, t-\tau_\mathrm{in})\,\mathrm{d}\tau_\mathrm{in}. \tag{5}$$

The main assumption required for the transfer function model to work is the applicability of the principle of linear superposition, which states that the response of a system to a string of impulses is just the sum of the responses to the individual impulses. This presupposes steady state hydraulic conditions.

To apply the transfer function theory to describe the solute mass evolution at an irrigation well in response to solute recycling, re-introduction of the extracted solute mass flux $J_\mathrm{p}(t)$ back into the system has to be described by a transfer function. The well response $J_\mathrm{p}(t)$ in the 'recycling source' in Eq. (2) can be obtained by means of Eq. (5), on condition that a transfer function is found which describes the transformation of a mass signal released at $\boldsymbol{x}$ in response to solute recycling.

In the following, a *recycling transfer function* (RTF) is formulated by means of the travel time PDF $g_t^{\gamma}(t)$ between the recycling point $\boldsymbol{x}$ and the well $\boldsymbol{x}'$. Subsequently, the travel time PDF $g_t^{\gamma}(t)$ in Eq. (5) is replaced by the RTF, yielding the solute mass evolution at the well $J_{\mathrm{p}}(t)$ in response to solute recycling, necessary to define the 'recycling source' in Eq. (1).

4.1. The recycling transfer function (RTF)

As indicated above, the mass-normalised transient well response to solute recycling resulting from a narrow pulse at the recycling point $\boldsymbol{x}$ will be referred to as the *recycling transfer function* (RTF) $g_{\mathrm{in}}^{\gamma}(t)$. The RTF can be obtained step-by-step, by describing the well responses to n possible recycling cycles separately, thereby assuring that all possible solute breakthroughs at the well are taken into account.

According to Eq. (3), the response at the well to a narrow pulse released at the recycling point $\boldsymbol{x}$ corresponds to the travel time PDF $g_t^{\gamma}(t)$. When solute recycling takes place and the assumption is made that there is no time-lapse between solute-extraction and re-introduction, the well response $g_t^{\gamma}(t)$ will be re-introduced into the system on the recycling point $\boldsymbol{x}$, forming the continuation of the input signal. This process leads to self-convolution of the travel time PDF $g_t^{\gamma}(t)$, since the mass input signal at $\boldsymbol{x}$ equals the well response at $\boldsymbol{x}'$. A solute that has been recycled twice, has transited the flow path between $\boldsymbol{x}$ and $\boldsymbol{x}'$ twice (symbolised by the index 2γ). The travel time PDF corresponding to the response at the well of all solutes that have transited between $\boldsymbol{x}$ and $\boldsymbol{x}'$ twice describes the second recycling cycle PDF $g_t^{2\gamma}(t)$ and is obtained by self-convolution of the travel time PDF $g_t^{\gamma}(t)$ as follows:

$$g_t^{2\gamma}(t) = \int_0^t g_t^{\gamma}(t-u) g_t^{\gamma}(u)\,\mathrm{d}u = g_t^{\gamma}(t) * g_t^{\gamma}(t). \tag{6}$$

The relationship in Eq. (6) is true for any multiple repetition of the transit between $\boldsymbol{x}'$ and $\boldsymbol{x}$ and can therefore be used to express any recycling cycle PDF $g_t^{n\gamma}(t)$ by means of the travel time PDF $g_t^{\gamma}(t)$ between the recycling point $\boldsymbol{x}$ and the well $\boldsymbol{x}'$. The respective recycling cycle PDFs $g_t^{n\gamma}(t)$ can be expressed either in the time domain or in Laplace space, where a convolution integral reduces to a simple product, as follows:

where p [T^{-1}] is the Laplace variable and the angular over-scores describe the Laplace transformed functions. The resulting output signal of any recycling cycle yields the input signal of the following recycling cycle, which is reflected in the series of self-convolutions. The 0th recycling cycle PDF $g_t^{0\gamma}(t)$ indicates instantaneous recycling between the well and the recycling point $\boldsymbol{x}$ at the moment of the unit mass release at $t = 0$. The recycling cycle PDF $g_t^{n\gamma}(t)$ at a time τ yields the travel time contribution to the RTF that has transited between $\boldsymbol{x}$ and $\boldsymbol{x}'$ n-times. Hence, the RTF $g_{\mathrm{in}}^{\gamma}(t)$ can be written as sum of the contributions of all possible recycling cycles PDFs $g_t^{n\gamma}(t)$, $n = 0, 1, 2, \ldots, \infty$, shown in Eqs. (7) as follows:

$$g_{\mathrm{in}}^{\gamma}(t) = \sum_{n=0}^{\infty} g_t^{n\gamma}(t). \tag{8}$$

Or, expressed in Laplace space:

$$\hat{g}_{\mathrm{in}}^{\gamma}(p) = \sum_{n=0}^{\infty} \hat{g}_t^{\gamma}(p)^n = \frac{1}{1-\hat{g}_t^{\gamma}(p)}, \quad |\hat{g}_t^{\gamma}(p)| \leqslant 1. \tag{9}$$

The RTF $g_{\mathrm{in}}^{\gamma}(t)$ reflects a travel time distribution consisting of solutes that have been recycled different numbers of times (Fig. 2). Hence, for a given travel time τ_{life} represented in the RTF $g_{\mathrm{in}}^{\gamma}(t)$, no difference is made in the number of times a solute has been recycled. As an example, a solute that has been recycled once has a given probability of arriving at the well before τ_{life}, while a solute that has been recycled twice will have suffered an additional convolution with the travel time PDF $g_t^{\gamma}(t)$ and thus have a smaller probability of arriving before τ_{life}. In the RTF $g_{\mathrm{in}}^{\gamma}(t)$, the probability of arriving before τ_{life} will consist of the lumped probability of all possible recycling cycles of arriving before τ_{life}. The main difference between the travel time PDF $g_t^{\gamma}(t)$ and the RTF $g_{\mathrm{in}}^{\gamma}(t)$ is that one and the same solute in the RTF will represent multiple solute life times, whereas in the PDF $g_t^{\gamma}(t)$ every initially released solute will represent only one life time. Hence, the RTF $g_{\mathrm{in}}^{\gamma}(t)$ cannot be considered in terms of one PDF, but has to be regarded as a multitude of superimposed PDFs.

Fig. 2 shows the RTF $g_{\mathrm{in}}^{\gamma}(t)$ and the recycling cycle PDFs $g_t^{n\gamma}(t)$ of several recycling cycles for a 1-D closed system (cf. Fig. 1 with $Q_{\mathrm{D}} = 0$) where solute recycling takes place on a single point $\boldsymbol{x}$ only. For a given solute

Recycling cycle PDFs

	Time domain	Laplace space
0th recycling cycle:	$g_t^{0\gamma}(t) = \delta(t)$	$\hat{g}_t^{0}(p) = 1$
1st recycling cycle:	$g_t^{1\gamma}(t) = g_t^{\gamma}(t)$	$\hat{g}_t^{1\gamma}(p) = \hat{g}_t^{\gamma}(p)^1$
2nd recycling cycle:	$g_t^{2\gamma}(t) = g_t^{\gamma}(t) * g_t^{\gamma}(t)$	$\hat{g}_t^{2\gamma}(p) = \hat{g}_t^{\gamma}(p)^2$
nth recycling cycle:	$g_t^{n\gamma}(t) = g_t^{\gamma}(t) * g_t^{\gamma}(t) * \cdots * g_t^{\gamma}(t)$	$\hat{g}_t^{n\gamma}(p) = \hat{g}_t^{\gamma}(p)^n$

(7)

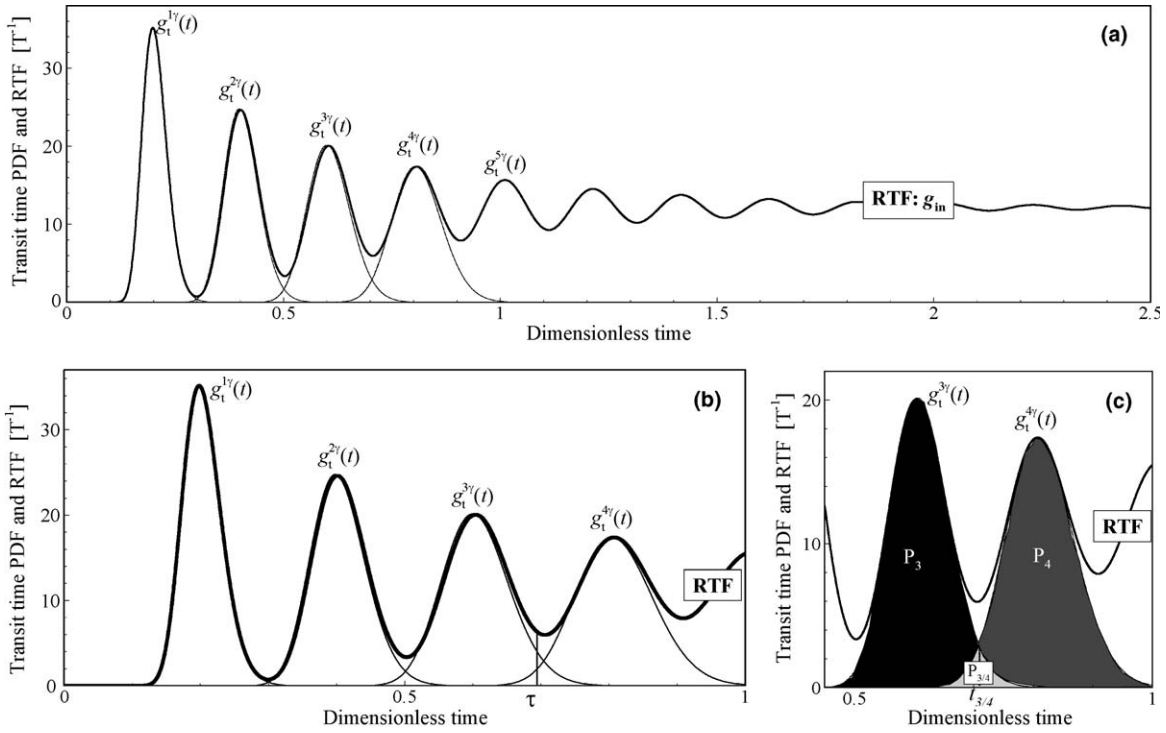

Fig. 2. Graphical representation of the advective–dispersive solute recycling process in a closed system, showing the superposition of the recycling cycle PDFs, corresponding to the solute life time contributions of different recycling cycles adding up to the recycling transfer function RTF $g_{in}^{\gamma}(t)$. (a) Showing the RTF as well as four recycling cycle PDFs. (b) Close-up of the four recycling cycle PDFs $g_t^{n\gamma}(t)$, $n = 1,2,3,4$, with indicated solute life time τ to which mainly $g_t^{3\gamma}(t)$ and $g_t^{4\gamma}(t)$ contribute. (c) Close-up of $g_t^{3\gamma}(t)$ and $g_t^{4\gamma}(t)$ with indicated surfaces corresponding to recycling probabilities.

arrival or life time τ, indicated on Fig. 2b, the contribution from the first and the second recycling cycle PDFs $g_t^{1\gamma}(t)$ and $g_t^{2\gamma}(t)$ tend towards zero, while the contributions from the third and fourth recycling cycles, $g_t^{3\gamma}(t)$ and $g_t^{4\gamma}(t)$ add up to the RTF $g_{in}^{\gamma}(t)$. In Fig. 2c, the surface P_3 represents the probability of a solute within the third recycling cycle of having a solute life time τ smaller than the solute life time within the fourth recycling cycle: in other words, it is the probability of solutes in the third recycling cycle of not being 'overtaken' by solutes of a higher order cycle. P_4 represents the probability of solute life times in the fourth recycling cycle being longer than the solute life times in all lower order recycling cycles. $P_{3/4}$ is the probability of solutes within either the third or the fourth recycling cycle of having the same solute life time: these are the solutes which are 'just about' to overtake or to be overtaken. The time $\tau_{3/4}$ corresponds to the solute life time for which the contributions to the RTF of the two neighbouring PDFs are identical. The more a system is dispersive or the shorter the travel times are to the extraction well, the more likely it is that solutes which have already been recycled n times will 'overtake' solutes of a lesser recycling order. The 'overtaking' leads to the homogenisation and therefore to the smoothening of the response at long times, only possible in dispersive systems.

The RTF $g_{in}^{\gamma}(t = \infty)$ at long times tends towards a constant value (Fig. 2a) which corresponds to the inverse of the mean travel time between the recycling point and the well (first moment of the travel time PDF $g_t^{\gamma}(t)$, see Appendix A, (A.4)), reflecting the recycling frequency in a perfectly homogenised closed system. The higher the recycling frequency is, the higher the concentration will be in response to solute recycling, since the same amount of solute is captured in a smaller recycling circuit.

In open systems, characterised by $P(\boldsymbol{x}) < 1$, the RTF $g_{in}^{\gamma}(t)$ at long times will drop to zero, since the initially released solute mass will eventually leave the recycling circuit.

In the same way as the travel time PDF $g_t^{\gamma}(t)$ is a transfer function reflecting the transformation of an input signal released at $\boldsymbol{x}$ by the time of arrival at a well $\boldsymbol{x}'$, the RTF $g_{in}^{\gamma}(t)$ is a transfer function that describes how a solute signal released at $\boldsymbol{x}$ will be transformed by the process of solute recycling.

4.2. The well solute mass response $J_p(t)$

To obtain the well solute mass response $J_p(t)$, the travel time PDF $g_t^{\gamma}(t)$ in Eq. (5) is replaced by the RTF $g_{in}^{\gamma}(t)$ and convoluted with the solute mass flux $I(t)$ captured by the well from the boundaries, corresponding to the solute signal that enters the recycling circuit. In Laplace space, the convolution integral in Eq. (5) simplifies to the following product, using Eq. (9) for the RTF:

$$\hat{J}_{\mathrm{p}} = \hat{I}\hat{g}^{\gamma}_{\mathrm{in}}(p) = \hat{I}\sum_{n=0}^{\infty}\hat{g}^{\gamma}_{t}(p)^{n} = \hat{I}\frac{1}{1-\hat{g}^{\gamma}_{t}(p)}. \tag{10}$$

Eq. (10) yields the solute mass response at a well $\hat{J}_{\mathrm{p}}$ for arbitrary advective–dispersive systems and solute mass flux $\hat{I}$ captured by the well from the boundaries. Inversion of Eq. (10) allows definition of the distributed transient 'recycling source' term RS(t) in Eq. (2), which in turn allows direct transient simulation of solute recycling, i.e., without coupling the extracted solute mass flux from the wells to a distributed solute source on irrigation surfaces in a time-stepping procedure.

Assuming steady state conditions with respect to the solute mass flux along the boundary and neglecting the dispersive transport component along the boundary, the solute mass flux I [M T^{-1}] captured by the well from the inflow boundary is considered to be constant (in Laplace space written as $\hat{I} = I/p$). Then, Eq. (10) can be reformulated as follows:

$$p\hat{J}_{\mathrm{p}} = I\frac{1}{(1-\hat{g}^{\gamma}_{t}(p))}, \quad I = \int_{\Gamma^{-}} PC_0\mathbf{q}\cdot\mathbf{n}. \tag{11}$$

Integration over the inflow boundaries Γ^{-} of the product of the solute mass flux ($C_0\mathbf{q}\cdot\mathbf{n}$) and the capture probability field P yields the constant lateral solute mass flux I captured by the well from the boundaries. According to the definition of the Laplace transform, Eq. (11) corresponds to the following expression in the time-domain (for $t > 0$):

$$\frac{\partial J_{\mathrm{p}}}{\partial t} = Ig^{\gamma}_{\mathrm{in}}(t). \tag{12}$$

Eq. (12) shows that the RTF $g^{\gamma}_{\mathrm{in}}(t)$ scaled by the constant solute mass flux I equals the first time-derivative of the solute mass response $J_{\mathrm{p}}(t)$ at the well. Hence, the solute mass evolution at an irrigation well is governed by two factors: (1) the solute mass captured by the well from the boundaries I, which is a system characteristic, and (2) the RTF $g^{\gamma}_{\mathrm{in}}(t)$ which in turn governs how re-distribution of the imported solutes will affect groundwater salinisation, being the spatial factor. For a given solute mass flux captured from the boundaries, spatial variations in solute recycling, reflected in differences in the RTFs, will lead to different groundwater salinisation evolutions. Hence, spatial variations in irrigation schemes will not only induce spatial variations in groundwater salinisation but also govern the degree of salinisation.

Fig. 3 shows the flow rate normalised well solute mass fluxes (i.e., well concentrations, dashed lines with circles) and the corresponding RTFs $g^{\gamma}_{\mathrm{in}}(t)$ (full lines) for solute recycling at two relative spatial coordinates ($x = 0.2$ in Fig. 3a and c; and $x = 0.8$ in Fig. 3b and d) in a 1-D closed system ($P(\boldsymbol{x}) = 1$, Fig. 3a and b) and open system ($P(\boldsymbol{x}) < 1$, Fig. 3c and d). A lateral inflow boundary is located at $x = 0$ with $C(x = 0, t) = 1$, and an extraction well at $x = 1$. According to Eq. (12), the RTFs $g^{\gamma}_{\mathrm{in}}(t)$ shown in Fig. 3a–d were scaled by the lateral constant solute mass flux I, then integrated and normalised by the constant well extraction rate Q_{p} to obtain the transient well concentration evolutions $C_{\mathrm{p}}(t)$ (dashed lines with circle symbols). The transient well concentration evolutions $C_{\mathrm{p}}(t)$ compare well with the results from numerical transient simulations run with solute recycling in a time-stepping procedure (bold lines). Hence, simulation of the travel time PDF $g^{\gamma}_{t}(t)$, followed by a n-fold convolution and scaling with the solute mass flux I at the well, allows definition of the transient 'recycling source' in Eq. (1), using the relationship established in Eq. (12).

In closed systems (Fig. 3a and b), the solutes that are captured by the well from the boundary are trapped in the recycling circuit. Therefore, the system concentration will increase infinitely. In open systems (Fig. 3c and d), in which a fraction of the solutes leave the recycling circuit, the RTF $g^{\gamma}_{\mathrm{in}}(t)$ will tend towards zero at long times. In such settings, the extracted solute mass flux $J_{\mathrm{p}}(t)$ will stabilise at long times, reflecting that the solute mass loss from the recycling circuit equals the solute mass flux entering the recycling circuit (Fig. 3c and d).

As illustrated in Fig. 3c and d, open systems attain a steady state solute mass flux $J_{\mathrm{p}}(t)$ at long times ($t \to \infty$). To determine the steady state solute mass flux in Laplace space, the limit value of $p\hat{J}_{\mathrm{p}}$ for $p = 0$ is sought (cf. Appendix B, (B.3)):

$$J_{\mathrm{p}}(t = \infty) = \lim_{p\to 0} p\hat{J}_{\mathrm{p}}. \tag{13}$$

Combining Eq. (11) and Eq. (13) yields:

$$J_{\mathrm{p}}(t = \infty) = \frac{I}{1 - \lim_{p\to 0}\hat{g}^{\gamma}_{t}(p)}. \tag{14}$$

According to the definition of the Laplace transform, $\lim_{p\to 0}\hat{g}^{\gamma}_{t}(p)$ corresponds to the 0th moment of the travel time PDF $g^{\gamma}_{t}(t)$, i.e., the capture probability $P(\boldsymbol{x})$ as defined in Eq. (4):

$$\lim_{p\to 0}\hat{g}^{\gamma}_{t}(p) = \lim_{p\to 0}\int_{0}^{\infty} \mathrm{e}^{-pt}g^{\gamma}_{t}(t)\,\mathrm{d}t = \int_{0}^{\infty} g^{\gamma}_{t}(t)\,\mathrm{d}t = P(\boldsymbol{x}). \tag{15}$$

Introducing Eq. (15) into Eq. (14) yields:

$$J_{\mathrm{p}}(t = \infty) = \frac{I}{1 - P(\boldsymbol{x})}. \tag{16}$$

Applying Eq. (16) to closed systems, which are defined by a capture probability $P(\boldsymbol{x}) = 1$, yields a solute mass flux $J_{\mathrm{p}}(t = \infty) = \infty$ (cf. Fig. 3a and b).

Re-formulating Eq. (16) and denoting $J_{\mathrm{p}}(t = \infty)$ with J_{p} leads to:

$$J_{\mathrm{p}} = I + P(\boldsymbol{x})J_{\mathrm{p}}. \tag{17}$$

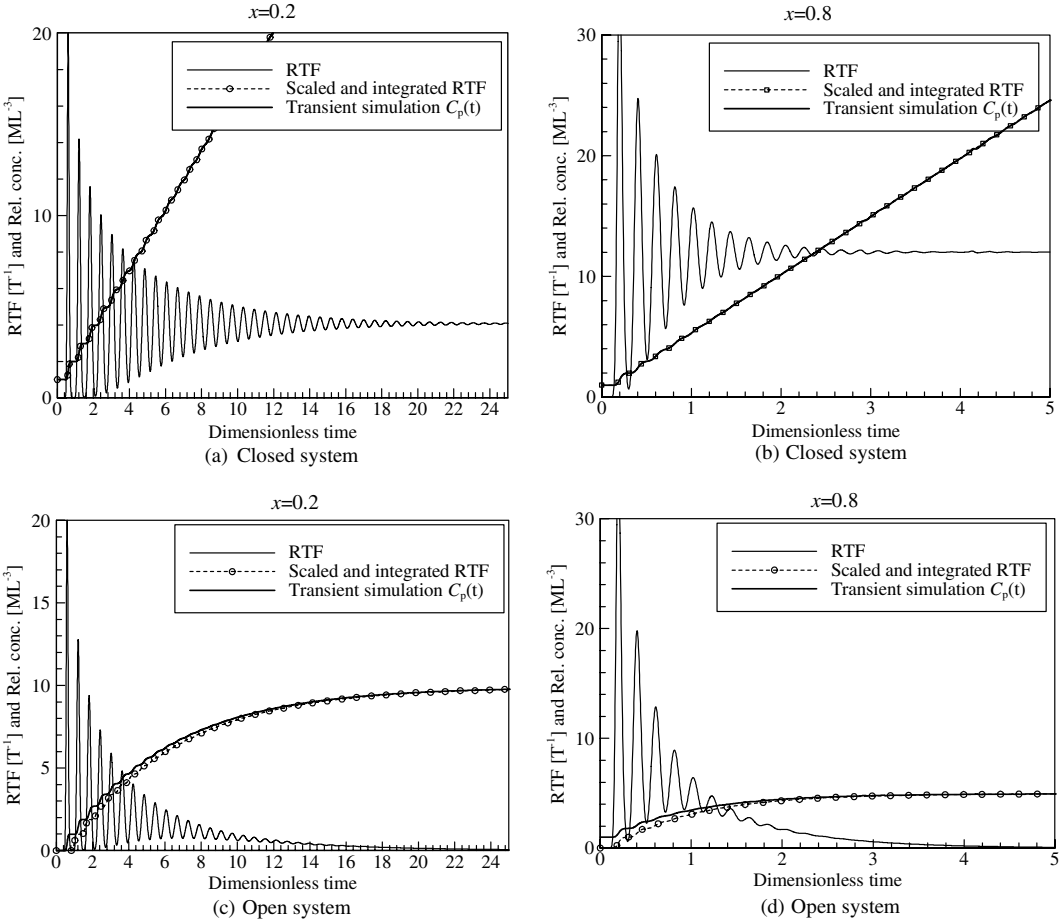

Fig. 3. Transient well concentration responses $C_p(t)$ (dashed lines with circles) obtained from scaling the RTFs $g_{in}^{\gamma}(t)$ (full lines) by the lateral solute mass flux I, time-integrating and normalising with the extraction rate Q_p for different relative spatial coordinates ($x = 0.2$ and $x = 0.8$) in a 1-D closed and open system with an extraction well located at $x = 1$. (a) and (b): Closed systems with $P(\boldsymbol{x})$=1, solute recycling at spatial coordinates $x = 0.2$ (a) and 0.8 (b), respectively. (c) and (d): Open systems with $P(\boldsymbol{x}) = 0.9$ solute recycling at spatial coordinates $x = 0.2$ and $P(\boldsymbol{x}) = 0.8$ solute recycling at $x = 0.8$ respectively, showing that the RTFs $g_{in}^{\gamma}(t)$ drop to zero and the well concentration $C_p(t)$ stabilises at long times.

To avoid evaluation of the capture probability $P(\boldsymbol{x})$ with an adjoint simulation [22,31], the solute mass flux at the well J_p can also be described as a perfect mixture of fractions f_i, originating from i different sources (i.e., from the different boundaries and from the irrigation plots, etc.). For the case that the flow rate at the well Q_p consists of only two components, the lateral inflow boundary contributes to the extraction rate with a fraction f_0 and the irrigation plot infiltration with a fraction f^*, such that $f^* + f_0 = 1$. With $Q_i = f^* Q_p$ being the deep percolation on the irrigation plot with the concentration $C^* = (C_p Q_p)/Q_i$, and C_0 the concentration along the boundary (Fig. 1). The steady state solute mass flux at the well J_p can then be expressed as follows:

$$J_p = Q_p(f^* C^* + f_0 C_0) = Q_p\left(f^* \frac{Q_p}{Q_i} C_p + f_0 C_0\right)$$
$$= J_p f^* \frac{Q_p}{Q_i} + I. \tag{18}$$

Re-formulating Eq. (18) yields:

$$J_p = \frac{I}{1 - f^* \frac{Q_p}{Q_i}}. \tag{19}$$

Eq. (19) is equivalent to Eq. (16) and shows the following relationship:

$$P(\boldsymbol{x}) = f^* \frac{Q_p}{Q_i} \tag{20}$$

Eq. (20) shows that the capture probability $P(\boldsymbol{x})$ equals the flow rate fraction f^* at the well derived from the irrigation point $\boldsymbol{x}$, scaled by the concentration increase induced by evaporative losses (Q_p/Q_i). Hence, the steady state solute mass flux at the well $J_p(t = \infty)$ can either be obtained from the capture probability $P(\boldsymbol{x})$ of the irrigation plot, using Eq. (16), or from the flow rate fraction f^* at the well derived from the recycling point $\boldsymbol{x}$, using Eq. (19).

However, describing the solute recycling process for steady state conditions directly by considering the different fractions (Eq. (19)) does not yield any information on the transient behaviour of the process, while the

expression found for the solute mass flux at the well in Eq. (16) resulted from the previous transient description of the solute recycling process, based on the transfer function theory.

The advantage of using the capture probability $P(\boldsymbol{x})$ in Eq. (16) may be considerable for optimisation purposes. With one single adjoint simulation, the well capture probability field can be simulated and the capture probability $P(\boldsymbol{x})$ of the irrigation plot in Eq. (16) can be optimised, i.e., the minimal value can be sought to obtain a minimal 'recycling source' in Eq. (2) without any further simulations. This only holds if the hypothesis can be made that the hydraulic field remains unchanged although the irrigation plot location is moved.

5. Direct simulation of solute recycling

To obtain the distributed 'recycling source' in the ADE, the extracted solute mass flux $J_p(t)$ in Eq. (10), corresponding to a convolution integral in the time-domain, is distributed over the irrigation plot surface Δ [L^2], according to Eq. (2) (or in the irrigation volume Δ [L^3] in a 3-D system). With a constant solute mass flux I captured by the well from the boundaries, Eq. (1) can be written with 'recycling source' RS(t) as follows:

$$\frac{\partial e\phi C}{\partial t} = -\nabla\cdot(e\mathbf{q}C - \phi e\mathbf{D}\nabla C) + \underbrace{\frac{I}{\Delta}\int_0^t g_{\mathrm{in}}^{\gamma}(\tau_{\mathrm{in}})\,\mathrm{d}\tau_{\mathrm{in}}}_{\mathrm{RS}(t)} \quad \text{on } \Delta, \tag{21}$$

elsewhere, RS(t) = 0.

The time-dependent 'recycling source' RS(t) in Eq. (21) can be constructed in a pre-processing stage. This requires simulation of the travel time PDF $g_i^{\gamma}(t)$ followed by n-fold convolution to obtain the RTF $g_{\mathrm{in}}^{\gamma}(t)$ and scaling with I prior to integration over time (cf. Fig. 3). Depending on the problem to be solved, this pre-processing stage may be more or less time-consuming. However, given hydraulic steady state conditions, this approach allows direct simulation of transient solute recycling with standard simulation codes.

5.1. Solute recycling potential

The maximum groundwater salinisation or salinisation potential in response to solute recycling for a given hydraulic setting and exploitation scheme is obtained by introducing the steady state solute mass flux $J_p(t=\infty)$, as shown in Eq. (16) or in Eq. (19), in the 'recycling source' in Eq. (21).

Since solute recycling takes place on a zone Δ, the capture probability $P(\boldsymbol{x})$ of the irrigation point in Eq. (16) is not related to a single recycling point $\boldsymbol{x}$ only, but to all points $\boldsymbol{x}$ within the irrigation plot Δ. Using Eq. (17), we can formulate the solute mass balance for the irrigation well for the case of re-distribution on an irrigation surface Δ as follows:

$$J_p = I + \frac{J_p}{\Delta}\int_{\Delta} P\,\mathrm{d}\Delta \tag{22}$$

The second term in Eq. (22) is the average capture zone probability over the irrigation plot ($\overline{P}(\Delta) = \frac{1}{\Delta}\int_{\Delta} P\,\mathrm{d}\Delta$) multiplied by J_p. Introducing the average capture probability $\overline{P}(\Delta)$ into Eq. (16), dividing it by the irrigation plot surface Δ, and introducing it in Eq. (1) as 'recycling source' RS, leads to the steady state form of the ADE accounting for solute recycling:

$$0 = -\nabla\cdot(e\mathbf{q}C - e\phi\mathbf{D}\nabla C) + \frac{I}{\Delta(1-\overline{P}(\Delta))}. \tag{23}$$

Eq. (23) with its constant 'recycling source' allows direct simulation of solute recycling in arbitrary systems for long times. The salinity distribution obtained from solving Eq. (23) yields the *solute recycling potential* or spatial recycling vulnerability of the system, being a measure of the groundwater salinisation a system is heading towards for a given exploitation and irrigation scheme in response to solute recycling. Since this steady state approach is computationally undemanding, multiple simulations can be carried out, for instance, to evaluate the impact of different irrigation schemes, or to identify potentially vulnerable areas or in view of optimisation purposes and stochastic modelling.

The only prerequisite to solve Eq. (23) is the average capture probability $\overline{P}(\Delta)$, which can be obtained with one single adjoint simulation [10,22,31] and subsequent calculation of the average over the irrigation area, or by determining the different flow rate fractions f_i^* in foreward simulations, according to Eqs. (18) and (19).

The adjoint or reversed flow field equation to be solved can be written as follows:

$$0 = e\mathbf{q}\cdot\nabla P + \nabla\cdot e\phi\mathbf{D}\nabla P, \tag{24}$$

with the boundary conditions,

$$\begin{aligned} P &= 1 \quad \text{on } \Gamma_p \text{ (well boundary)},\\ P &= 0 \quad \text{on } \Gamma^+ \text{ (discharge areas)}. \end{aligned} \tag{25}$$

Fig. 4 shows two results of the same 2-D horizontal, homogeneous, finite element model [10] with an extraction well at the coordinates (200/175). Flow is directed from east to west and a constant concentration of $C_0 = 1$ is imposed along the eastern limit. Fig. 4a shows a simulation result neglecting solute recycling, and in Fig. 4b, Eq. (23) was solved for the same system, assuming that irrigation takes place on the entire domain. The regional concentration gradient can be seen to be the opposite for the two cases. In Fig. 4a, the dilution effect of infiltration increases from east to west, while the concentration increases from east to west in Fig. 4b.

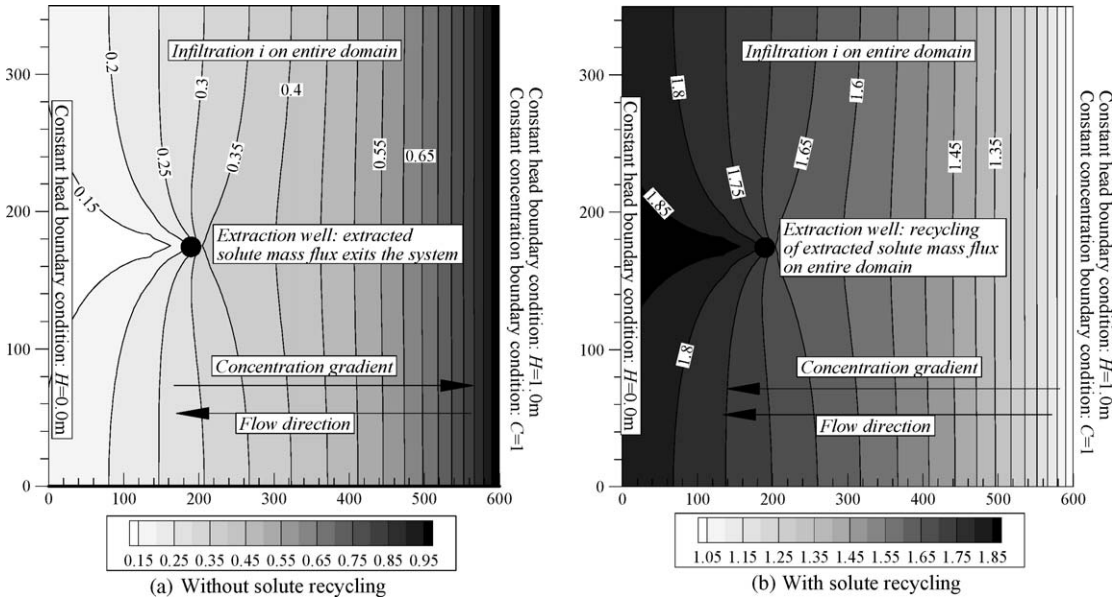

Fig. 4. Concentration distributions in a 2-D horizontal, homogeneous finite element model with an extraction well at coordinate (200/175). The flow is directed from east to west and a constant concentration of $C_0 = 1$ is imposed along the eastern limit. (a) Concentration distribution for steady state simulation without solute recycling. (b) Concentration distribution for steady state simulation according to Eq. (23) with solute recycling.

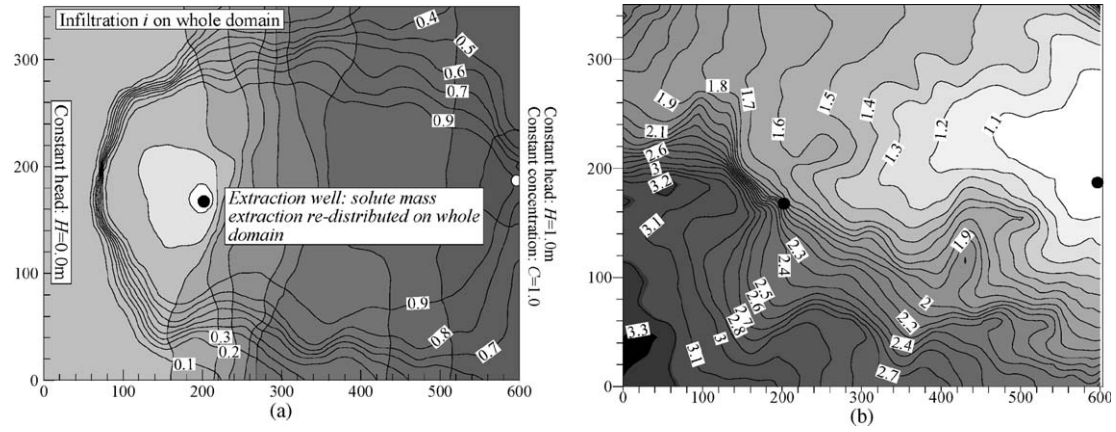

Fig. 5. 2-D horizontal, heterogeneous finite element model: (a) Head distribution (grey-scale) and iso-contours of capture zone probability field as full lines. (b) Comparison of concentration distribution of transient transport simulation with step-wise solute return flow (full lines) with direct steady state evaluation (grey-scale) obtained by solving Eq. (23). Extraction well located at (200/175).

Fig. 5 shows the concentration distribution obtained with a direct finite element simulation with solute recycling (grey scale) in a heterogeneous 2-D horizontal domain, applying Eq. (23) to a slightly different hydraulic setting than shown in Fig. 4 (i.e., with an injection point as inflowing boundary in the east). This is compared to the result from a transient simulation with solute recycling (full lines), in which the extracted solute mass flux was evaluated in a time-stepping procedure. The CPU requirements for the transient simulation was several orders of magnitude higher than those required using Eq. (23). The slight differences in the simulation results may be due to the fact that complete steady state was not attained in the transient simulation. The concentration distribution resulting from solute recycling on the entire domain is very heterogeneous, forming patch-like zones with high salinities. The down-stream areas are most affected, corresponding to where the fraction of irrigation return flow contained in the flow rate is highest.

Fig. 6 shows a 2-D homogeneous vertical system with solute recycling on the surface. In this case, the average capture zone probability field has to be integrated over the recycling length L. The 'recycling source' in Eq. (23) can then be written as follows:

$$\frac{J_p}{L} = \frac{I}{L(1-\overline{P}(L))}, \tag{26}$$

where $\overline{P}(L) = \frac{1}{L}\int_{\Gamma_{inf}} P\,dl$ is the average capture zone probability and Γ_{inf} is the recycling surface. Since the

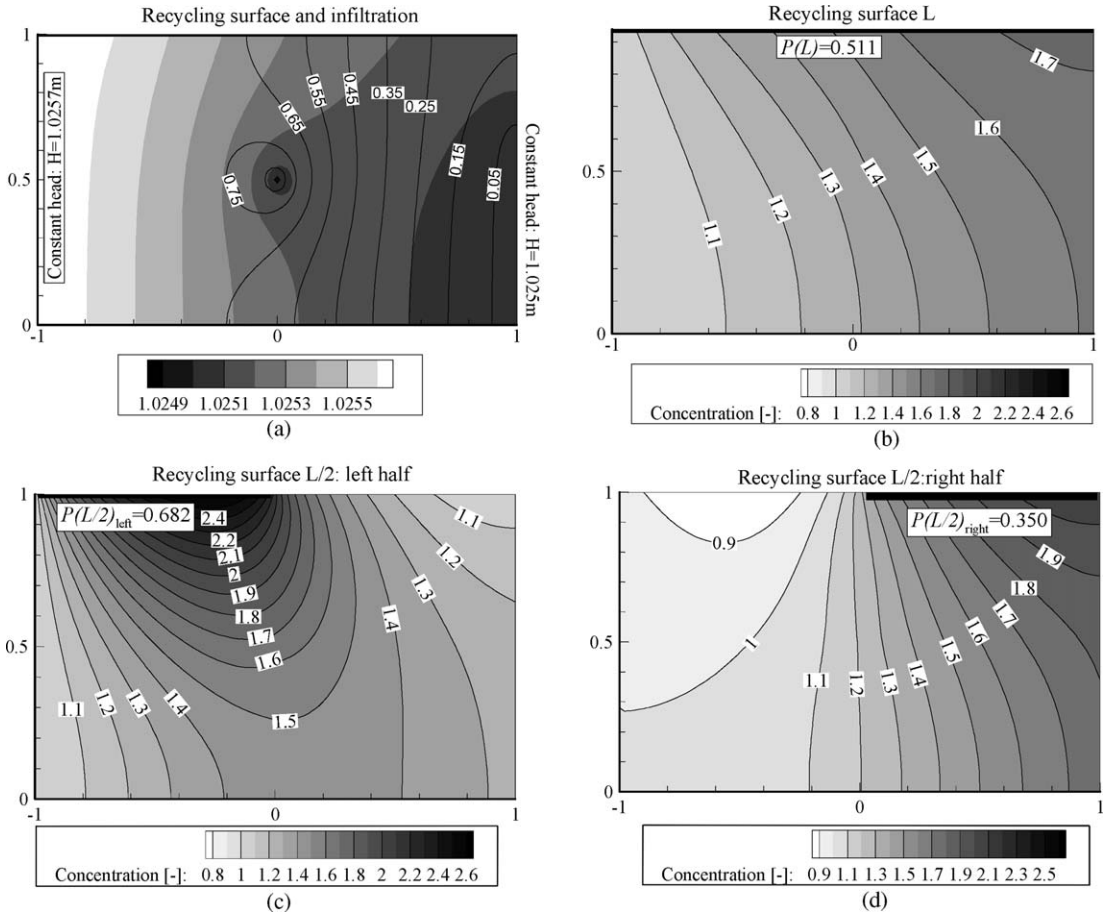

Fig. 6. 2-D vertical, homogeneous finite element model showing: (a) Boundary conditions and hydraulic head distribution (grey-scale) and the capture zone probability field (iso-lines); simulations run with dispersivities $\alpha_L = 0.001$ m and $\alpha_T = 0.01$ α_L. (b) The concentration distribution resulting from solute re-distribution on the entire surface (L). (c) Concentration distribution resulting from solute re-distribution on the left half $(L/2)_{\text{left}}$. (d) Concentration distribution resulting from solute re-distribution on the right half of the surface $(L/2)_{\text{right}}$, while infiltration takes place homogeneously over the entire domain. Well location (0/0.5).

recycling zone in a 2-D vertical case is an edge, a line of 1-D finite elements (with all hydrodynamic parameters set to zero) was introduced in the model to avoid re-formulation of the problem and definition of a coupled boundary condition. Fig. 6 shows how solute recycling acts in the vertical dimension, creating a concentration inversion in Fig. 6c, but it also illustrates the impact of heterogeneous solute recycling. The maximum concentration obtained from recycling on the entire surface (Fig. 6b, $\overline{P}(L) = 0.516$) is smaller than in Fig. 6c, where recycling takes place on only the left half of the domain. Fig. 6c has the highest impact due to a higher average capture zone probability ($\overline{P}(L/2)_{\text{left}} = 0.682$ versus $\overline{P}(L/2)_{\text{right}} = 0.350$ in Fig. 6d) leading to a larger 'recycling source' in Eq. (26) and thus to higher concentrations.

A possible application of the steady state solute recycling simulation approach is to optimise irrigation plot locations or extraction rates, since the computational requirements are very small. As an example, if the extraction rate remains constant and the assumption is made that changing the position of the irrigation plot will not affect the hydraulic conditions of the system, one single backward simulation is sufficient to evaluate the average capture zone probability of any potential irrigation zone $\overline{P}(\Delta)$, since the capture zone probability field remains unchanged. In this case, the only parameter to be minimised in the 'recycling source' described in Eq. (23) is $\overline{P}(\Delta)$. This can be obtained by carrying out the spatial integrations on the capture zone probability field over the different potential irrigation zones. Fig. 7 shows the same model as in Fig. 6. The rectangular zone (bold line) indicates the area within which irrigation with the extracted water may take place. However, the extracted groundwater is only sufficient to irrigate a smaller surface (sub-zone indicated as square). This sub-zone is then moved across the possible irrigation area to identify the location where irrigation will cause minimal groundwater degradation (i.e., where the average capture probability $\overline{P}(\Delta)$ is minimal). The irrigation plot location in Fig. 7c has the highest average capture probability leading to the highest concentrations, while

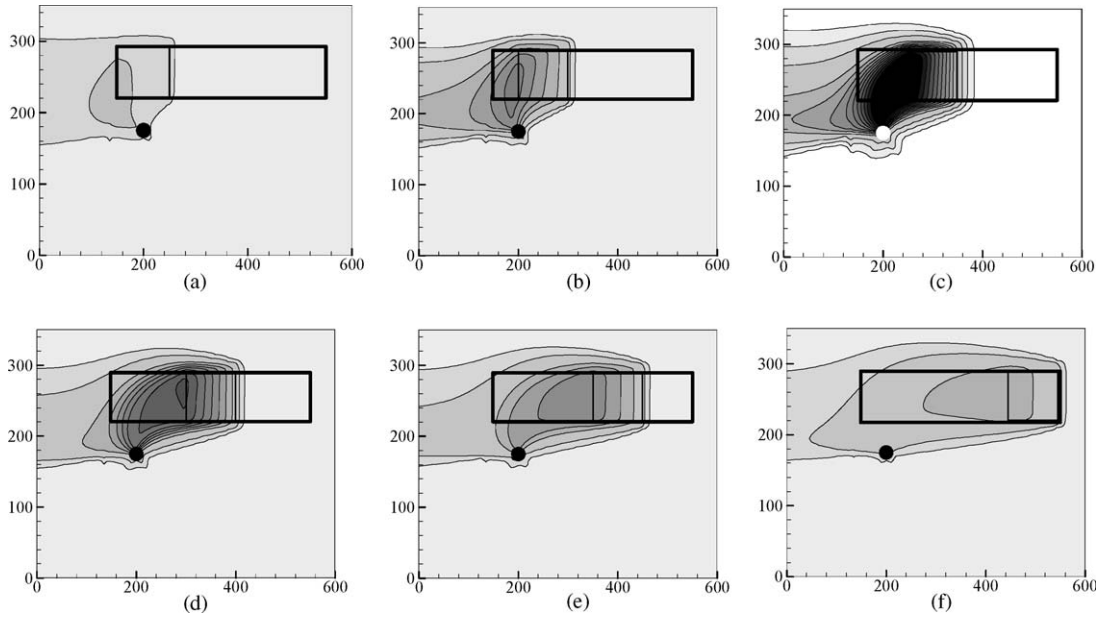

Fig. 7. Example of concentration distributions obtained by displacement of irrigation plot. Rectangular zone (bold line): possible irrigation surface. Square: Actual irrigation plot size to be located within the irrigation zone where mean capture zone probability field is minimal. (c) The highest concentrations are found for the irrigation plot with the highest mean probability of arriving at the well.

the sub-zone location in Fig. 7a has the minimal average capture probability for this setting.

5.2. Generalisation of the 'recycling source' to multiple wells and one irrigation plot

For several extraction wells that irrigate the same irrigation zone, the relationship for the extracted solute mass flux J_p, established in Eq. (17) is used to define the recycling source in Eq. (23). For a case with two extraction wells and one irrigation plot, defining $J_{ptot} = J_{p1} + J_{p2}$, the 'recycling source' can be written as follows:

$$\frac{J_{p1} + J_{p2}}{\Delta} = \frac{J_{ptot}}{\Delta} = \frac{(I_1 + \overline{P}_1 J_{ptot}) + (I_2 + \overline{P}_2 J_{ptot})}{\Delta}, \quad (27)$$

where J_{p1} and J_{p2} are the extracted solute mass fluxes from *wells* 1 and 2, respectively, with I_1 and I_2 the solute mass fluxes derived from the limits and $\overline{P}_1$ and $\overline{P}_2$ the respective average capture zone probabilities of each well. Developing Eq. (27) yields:

$$\frac{J_{ptot}}{\Delta} = \frac{I_1 + I_2}{\Delta(1 - (\overline{P}_1 + \overline{P}_2))}. \quad (28)$$

Generalising Eq. (28) to n extraction wells yields:

$$\frac{J_{ptot}}{\Delta} = \frac{\sum_{i=1}^{n} I_i}{\Delta\left(1 - \sum_{i=1}^{n} \overline{P}_i\right)}. \quad (29)$$

In Eq. (29), I_i is the lateral solute mass flux to the ith well and $\overline{P}_i$ is the corresponding average capture probability of well i.

Fig. 8a shows the same simulation result as in Fig. 5b. It is compared to a simulation carried out on the same domain with an additional extraction well (Fig. 8b): the two extraction wells together extract the same amount as the original single well in Fig. 8a. With the average capture probabilities $\overline{P}_1$, $\overline{P}_2$, the 'recycling source' was obtained, making use of Eq. (29). Comparing Fig. 8a and b reveals that the two-well configuration (Fig. 8b) extracting the same amount as in the single-well configuration (Fig. 8a) leads to a maximum relative concentration of $C_{max} = 2.60$ as compared to $C_{max} = 3.77$ in Fig. 8a, as a result of different hydraulic settings.

5.3. Generalisation of the 'recycling source' to multiple wells and multiple irrigation plots

To generalise the steady state 'recycling source' to several extraction wells and irrigation plots, the contributions to each well captured from other irrigation plots has to be taken into account. We denote J_{pk} the solute mass flux distributed on the kth irrigation plot which results from the solute mass extracted from i extraction wells. Eq. (17) has to be extended to include the solute mass contributions from the irrigation plots which are not irrigated by J_{pk}. The solute mass flux J_{pk} to be introduced onto the kth irrigation plot can then be written as a sum of contributions from all irrigation plots and the solute mass flux captured by the wells from the boundaries as follows:

$$J_{pk} = \sum_{i=1}^{n_k} \left(I_i + \sum_{j=1}^{m} J_{pj} P_i(\Delta_j) \right), \quad (30)$$

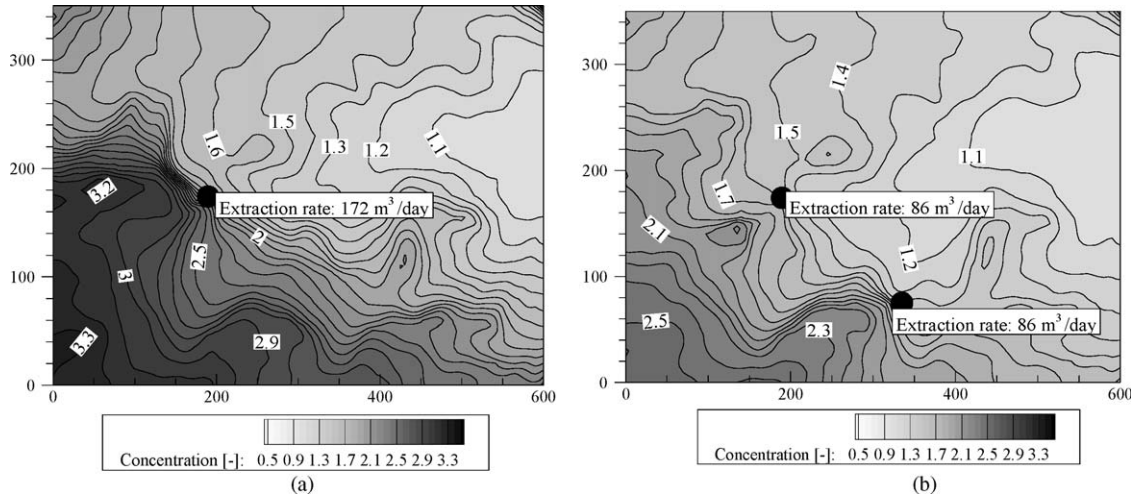

Fig. 8. (a) Concentration distribution as shown in Fig. 5b for one extraction well. (b) Concentration distribution obtained from simulation result with the same boundary conditions as in Fig. 8a except for an additional extraction well at coordinates (335/75): the two extraction wells together extract the same total amount as the one single well in (a). Model dimensions in meters.

where, m is the number of irrigation plots; n_k is the number of wells irrigating the kth plot; I_i is the solute mass flux captured by the ith well from the boundaries; J_{pj} is the solute mass flux recycled on the jth irrigation plot; $P_i(\Delta_j)$ is the average capture probability of the ith well with respect to the jth irrigation plot.

Developing Eq. (30) so that all terms of J_{pk} are on the left-hand side generates a system of m linear equations, which can be written in matrix form as follows:

$$\begin{bmatrix} 1-\sum_{i=1}^{n_1}P_i(\Delta_1) & -\sum_{i=1}^{n_1}P_i(\Delta_2) & \cdots & -\sum_{i=1}^{n_1}P_i(\Delta_m) \\ -\sum_{i=1}^{n_2}P_i(\Delta_1) & 1-\sum_{i=1}^{n_2}P_i(\Delta_2) & \cdots & -\sum_{i=1}^{n_2}P_i(\Delta_m) \\ \vdots & \vdots & \ddots & \vdots \\ -\sum_{i=1}^{n_m}P_i(\Delta_1) & -\sum_{i=1}^{n_m}P_i(\Delta_2) & \cdots & 1-\sum_{i=1}^{n_m}P_i(\Delta_m) \end{bmatrix} \times \begin{bmatrix} J_{p1} \\ J_{p2} \\ \vdots \\ J_{pm} \end{bmatrix} = \begin{bmatrix} \sum_{i=1}^{n_1}I_i \\ \sum_{i=1}^{n_2}I_i \\ \vdots \\ \sum_{i=1}^{n_m}I_i \end{bmatrix}. \quad (31)$$

With Eq. (31), the m steady state 'recycling sources' J_{pk} can be defined for any configuration of extraction wells and irrigation plots.

6. Concluding remarks

In the above exposition, the process of solute recycling was first described mathematically making use of the transfer function theory [19]. A *recycling transfer function* (RTF) was defined as the sum of the n-fold self-convolutions of the travel time PDF between the recycling point/zone. To obtain the well solute mass response at the irrigation well, the RTF was convoluted with the lateral solute mass flux captured by the well from the boundaries. The RTF describes how solutes are re-distributed within the system, while the lateral solute mass flux determines how solutes are introduced into the system. Hence, a concentration increase can only be observed, if solutes from other salinity sources exist (solute mass flux captured from the limits). This fact distinguishes the solute recycling salinisation process from other salinisation processes: solute recycling does not add any solutes to the system, it only leads to salinisation by re-distribution. The solute mass flux captured by the well from the boundaries concerns any solute source which may be present in the system. If, for instance, agrochemical additives enter the groundwater system, these can be accounted for by evaluating the solute mass flux captured by the wells from this salinity source, since they, too, will contribute to the solute recycling process. The same is true for any other source of salinity (e.g., geogenic salt, trapped seawater, etc.).

Prediction of the well solute mass response by means of the transfer function theory allowed definition of the 'recycling source' in the ADE in a pre-processing stage, generating the equivalent amount of solute mass that is being extracted from the irrigation well. In this way, coupling the extracted solute mass to the solute source within the simulation procedure, using a time-stepping procedure, can be avoided. Direct transient and steady state solute recycling simulations can thus be carried out.

At long times, the 'recycling source' is a function of the capture zone probability field and the solute mass flux from the boundaries. The concentration distribution obtained with the steady state 'recycling source' reflects the maximum spatial salinity distribution in response to solute recycling, reflecting the solute recy-

cling potential. Identification of the spatial vulnerability of a system towards salinisation by solute recycling using the proposed numerical approach is a step towards a process-based mapping procedure. Since the computational requirements are low for the steady state solute recycling simulations, a multitude of evaluations can be run, for instance, for optimisation purposes, such as the localisation of irrigation plots or well extraction rates to minimise aquifer salinisation.

The main assumption for the transfer function theory to work is hydraulic steady state condition. As long as steady state hydraulic conditions prevail, simulations accounting for the unsaturated zone can equally be carried out, which will simply result in a modification of the travel time PDF and of the RTF. However, before this approach can be applied, the validity of the assumptions underlying the transfer function theory for any given case have to be thoroughly assessed. As an example, in settings with a highly variable exploitation history, the assumption of hydraulic steady state condition might not be justified. Also, if density-dependent flow and transport is judged to be an important factor, this approach might not be appropriate.

Acknowledgements

The research described in this paper is supported in part by the European Community project SWIMED, Contract Nr. ICA3-CT-2002-10004. We would also like to thank O. Cirpka and the anonymous reviewers for their helpful comments.

Appendix A. Moment equations applied to the RTF

In Laplace space, the general definition of the nth moment can be written as follows for closed systems with $\lim_{p\to 0}\hat{g}_t^{\gamma}(p) = 1$ (i.e., $P(\boldsymbol{x}) = 1$):

$$\mu_n(\hat{g}_t^{\gamma}(p)) = (-1)^n \lim_{p\to 0} \frac{\partial^n \hat{g}_t^{\gamma}(p)}{\partial p^n}. \tag{A.1}$$

At long times, the RTF $\hat{g}_{\mathrm{in}}^{\gamma}(p)$ tends towards a constant value $g_{\mathrm{in}}(t=\infty) = m$ (Fig. 2). According to (B.3), the constant value at long times can be written as follows:

$$m = p\hat{m} = \lim_{p\to 0} p\hat{g}_{\mathrm{in}}^{\gamma}(p). \tag{A.2}$$

Making use of Eq. (9) for the definition of $\hat{g}_{\mathrm{in}}^{\gamma}(p)$, m can be expressed as follows:

$$m = \lim_{p\to 0} \frac{p}{1-\hat{g}_t^{\gamma}(p)}. \tag{A.3}$$

Which is undefined, since $\lim_{p\to 0}\hat{g}_t^{\gamma}(p) = 1$. Applying the rule of l'Hospital to overcome this, yields:

$$m = \lim_{p\to 0} \frac{p}{1-\hat{g}_t^{\gamma}(p)} = \lim_{p\to 0} \frac{1}{-\frac{\partial(\hat{g}_t^{\gamma}(p))}{\partial p}}. \tag{A.4}$$

Comparing (A.4) with the definition of the first moment given in (A.1) shows that the RTF $\hat{g}_{\mathrm{in}}^{\gamma}$ at long times tends towards the inverse of the first moment, corresponding to the mean travel time between the recycling point $\boldsymbol{x}$ and the well:

$$m = \frac{1}{\mu_1(\hat{g}_t^{\gamma}(p))}. \tag{A.5}$$

Appendix B. Derivation of long-time concentration in Laplace space

The constant concentration at long times $C(t=\infty)$ can be derived for any Laplace transformed solution $\hat{C}$ as follows:

$$\begin{aligned} C(t=\infty) &= \int_0^{\infty} \frac{\partial C}{\partial t}\,\mathrm{d}t + C(t=0) \\ &= \lim_{p\to 0}\left[\int_0^{\infty} \mathrm{e}^{-pt}\frac{\partial C}{\partial t}\,\mathrm{d}t + C(t=0)\right]. \end{aligned} \tag{B.1}$$

Making use of the following definition of the Laplace transform:

$$\int_0^{\infty} \mathrm{e}^{-pt}\frac{\partial C}{\partial t}\,\mathrm{d}t = p\hat{C} - C(t=0), \tag{B.2}$$

and introducing (B.2) into (B.1) yields:

$$C(t=\infty) = \lim_{p\to 0}(p\hat{C}). \tag{B.3}$$

References

[1] Al-Senafy M, Abraham J. Vulnerability of groundwater resources from agricultural activities in southern Kuwait. Agri Water Manage 2004;64:1–15.

[2] Aragüés R, Tanji KK, Quilez D, Alberto F, Faci J, Machin J, et al. Calibration and verification of an irrigation return flow hydrosalinity model. Irrigat Sci 1985;6:85–94.

[3] Barlow PM, Wagner BJ, Belitz K. Pumping strategies for management of a shallow water table: the value of the simulation-optimisation approach. Ground Water 1996;34(2):305–17.

[4] Beke GJ, Entz T, Graham DP. Long-term quality of shallow groundwater at irrigated sites. J Irrigat Drain Eng—ASCE 1993; 119(1):116–28.

[5] Beltrán JM. Irrigation with saline water: benefits and environmental impact. Agri Water Manage 1999;40:283–94.

[6] Bouwer H. Effect of irrigated agriculture on groundwater. J Irrigat Drain Eng—ASCE 1987;113(1):4–15.

[7] Bouwer H. Groundwater problems caused by irrigation with seawage effluent. J Environ Health 2000;63(3):17–20.

[8] Cardona A, Carillo-Rivera JJ, Huizar-Alvarez R, Graniel-Castro E. Salinization in coastal aquifers of arid zones: an example from Santo Domingo, Baja California Sur, Mexico. Environ Geol 2004; 45:350–66.

[9] Close ME. Effects of irrigation on water-quality of a shallow unconfined aquifer. Water Resour Bull 1987;23(5):793–802.
[10] Cornaton F. Deterministic models of groundwater age, life expectancy and transit time distributions in advective–dispersive systems. PhD thesis, University of Neuchâtel, Switzerland, 2004.
[11] Essaid HI. A multilayered sharp interface model of coupled freshwater and saltwater flow in coastal systems: model development and application. Water Resour Res 1990;26(7):1431–54.
[12] Gambolati G, Putti M, Paniconi C. Three-dimensional model of coupled flow and miscible salt transport. In: Bear J, Cheng AH-D, Sorek S, Ouazar D, Herrera I, editors. Seawater intrusion in coastal aquifers—concepts, methods and practices. Dordrecht: Kluwer Academic Publishers; 1999 [chapter 10].
[13] Goode DJ. Direct simulation of groundwater age. Water Resour Res 1996;32(2):289–96.
[14] Gordon E, Shamir U, Bensabat J. Optimal management of a regional aquifer under salinization conditions. Water Resour Res 2000;36(11):3193–203.
[15] Jury WA. Simulation of solute transport using a transfer function model. Water Resour Res 1982;18(2):363–8.
[16] Jury WA, Sposito G, White RE. A transfer function model of solute transport through soil, 1: Fundamental concepts. Water Resour Res 1986;22(2):243–7.
[17] Jury WA, Roth K. Transfer functions and solute movement through soil: theory and applications. Bosten, Cambridge, MA: Birkhäuser; 1990.
[18] Kim Y, Lee KS, Koh DC, Lee DH, Lee SG, Park WB, et al. Hydrogeochemical and isotopic evidence of groundwater salinisation in a coastal aquifer: a case study in Jeju volcanic island, Korea. J Hydrol 2003;270:282–94.
[19] Kolodny Y, Katz A, Starinsky A, Moise T, Simon E. Chemical tracing of salinity sources in Lake Kinneret (Sea of Galilee), Israel. Limnol Oceanograph 1999;44(4):1035–44.
[20] Konikow LF, Person M. Assessment of long-term salinity changes in an irrigated stream-aquifer system. Water Resour Res 1985; 21(11):1611–24.
[21] Milnes E, Renard P. The problem of salt recycling and seawater intrusion in coastal irrigated plains: an example from the Kiti aquifer (Southern Cyprus). J Hydrol 2004;288:327–43.
[22] Neupauer RM, Wilson JL. Adjoint method for obtaining backward-in-time location and travel time probabilities of a conservative groundwater contaminant. Water Resour Res 1999;35(11): 3389–98.
[23] Oster JD. The use of models in salinity assessment: steady-state rootzone salt balance. In: Tanji KK, editor. Agricultural salinity assessment and management. ASCE manuals and reports on engineering practice. American Society of Civil Engineers; 1990. p. 71.
[24] Oster JD. Irrigation with poor quality water. Agri Water Manage 1994;25(3):271–97.
[25] Pearce MW, Schumann EH. The impact of irrigation return flow on aspects of the water quality of the Upper Gamtoos Estuary, South Africa. Water SA 2001;27(3):367–72.
[26] Prendergast JB, Rose CW, Hogarth WL. Sustainability of conjunctive water use for salinity control in irrigated areas: theory and application to the Shepparton region, Australia. Irrigat Sci 1993;14:177–87.
[27] Sites W, Kraft GJ. Groundwater quality beneath irrigated vegetable fields in a north-central US sand plain. J Environ Qual 2000;29(5):1509–17.
[28] Strigter TY, Van Ooijen SPJ, Post VEA, Appelo CAJ, Carvahlo Dill AMM. A hydrogeological and hydrochemical explanation of the groundwater composition under irrigated land in a Mediterranean environment, Algarve, Portugal. J Hydrol 1998;208: 262–79.
[29] Stewart IT, Loague K. A type transfer function approach for regional-scale pesticide leaching assessments. J Environ Qual 1999;28:378–87.
[30] Tanji KK. A conceptual hydrosalinity model for predicting salt load in irrigation flows. In: Managing saline water for irrigation, Proc int conf on managing saline water for irrigation, 1977.
[31] Uffink GJM. Application of the Kolmogorov's backward equation in random walk simulation of groundwater contaminant transport. In: Kobus HE, Kinzelbach W, editors. Contaminant transport in groundwater. Rotterdam: Balkema; 1989. p. 283–9.
[32] Van Genuchten MTh, Dalton FN. Models for simulating salt movement in aggregated soils. Geoderma 1980;38:165–83.
[33] Van Schilfgaarde J. Drainage design for salinity control. In: Shainberg I, Shalhevet J, editors. Soil salinity under irrigation. Berlin, New York, Tokio: Springer-Verlag; 1984. p. 190–7.
[34] Vengosh A, Spivack A, Artzi Y, Avner A. Geochemical and boron, strontium and oxygen isotopic constraints on the origin of the salinity in groundwater from the Mediterranean coast of Israel. Water Resour Res 1999;35(6):1877–94.
[35] Vengosh A, Gill J, Davisson ML, Hudson GB. A multi-isotope (B, Sr, O, H and C) and age-dating (H-3, He-3 and C-14) study of groundwater from salinas Valley, California: Hydrochemistry, dynamics and contamination processes. Water Resour Res 2002; 38(1):1008.
[36] Voss CI. USGS SUTRA Code—History, practical use, and application in Hawaii. In: Bear J, Cheng AH-D, Sorek S, Ouazar D, Herrera I, editors. Seawater intrusion in coastal aquifers—concepts, methods and practices. Dordrecht: Kluwer Academic Publishers; 1999 [chapter 9].